Modulation Strategy to Minimise RMS and Peak Currents in Dual Active Bridge Converter

Dibakar Das
Department of Electrical Engineering
Indian Institute of Science
Bangalore, India
dibakard@iisc.ac.in

Kaushik Basu
Department of Electrical Engineering
Indian Institute of Science
Bangalore, India
kbasu@iisc.ac.in

***Abstract*—Optimal operation of dual active bridge (DAB) converters has been extensively researched in literature. The modulation parameters of the DAB converter are chosen to minimise a given objective function which can be the RMS or the peak of inductor current. This paper presents a comparison of the optimal rms current problem and the optimal peak current problem. For medium power operation, a closed-form solution is derived for the modulation parameters which leads to minimum RMS currents. It is observed that the solution is computationally demanding and hence not suitable for real-time implementation. A hybrid modulation strategy is proposed which achieves both optimal rms and peak currents and is simple to implement in real-time. Simulation and experimental results confirm the theoretical analysis.**

***Index Terms*—Dual Active Bridge, Soft switching, Optimal modulation, Ferrari Method**

I. Introduction

Dual active bridge (DAB) is a promising solution for DC-DC converters because of their several advantages such as galvanic isolation, bidirectional power flow capability and soft switching features leading to high efficiency and power density [1]. Due to their advantages, DAB converters have numerous applications in DC microgrids, electric vehicle charging and solid state transformers.

Dual active bridge converters are conventionally controlled through phase shift modulation [2] where H-bridge converters apply square waveforms to the windings of a high frequency transformer. A phase shift is introduced between the primary and secondary voltage waveforms for power transfer. However, this leads to large rms currents and hence losses in the system when the voltage conversion ratio is far from unity [3], [4]. Multiple degrees of freedom in modulation can be introduced for better performance in terms of rms current reduction and soft switching over a wide load range. In general, the triple phase shift (TPS) scheme has three degrees of freedom in modulation viz. the duty cycles of the square waveforms and the phase shift between them. Several attempts have been made in literature to devise an optimal modulation strategy with TPS which will lead to efficiency improvement [4]–[6]. In such problems, for a given power, voltage levels, switching frequency and the design parameters (transformer turns ratio and series inductance), the objective is to determine the optimal TPS modulation variables. Existing literature on optimal DAB modulation mainly focus on minimisation of either rms or the peak inductor current as they are directly related to the device stresses and losses of the converter.

The inductor rms current and current stress minimisation problems for dual active bridge converters have been extensively studied in literature [4]–[10]. The rms current minimisation problem considering ZVS constraints has been solved for the entire operating range of the converter in [5]. The solution however does not provide closed-form expressions for all the operating regions of the converter. Moreover, the optimal solution for rms current minimisation is complicated for real-time implementation. An optimal TPS modulation scheme for achieving minimum current stress with soft-switching is explored in [9]. However, fundamental approximation is used for the analysis which reduces the accuracy of the solution. The current stress minimisation problem with ZVS constraints is finally solved in [6], [11]. The rms current and peak current optimisation in general lead to different set of solutions since the objective function being minimised is different. A comparative study of these solutions and strategy for minimising both rms and peak current does not exist in literature.

Through a comparative study between the optimal solutions obtained for rms current and peak current minimisation, a hybrid modulation strategy is proposed which results in simplified implementation and overall minimisation of both rms and peak currents. In this paper, a closed form solution is also found for the medium power operation which gives minimum rms currents. The analysis is verified on a 4 kW experimental prototype.

The rest of the paper is organized as follows. Section II provides the description of the optimisation problem. The optimal rms and peak current solutions are discussed for various operating powers. A closed form solution for medium power operation is proposed which leads to minimum value of rms currents. A modulation strategy is then proposed which gives optimal rms and peak currents. Section III presents the simulation and experimental results. Section IV concludes the paper.

II. Analysis

Consider a dual active bridge converter with given voltage levels V_1, V_2, power rating P and switching frequency f_s

978-1-7281-5826-6/20/$31.00 ©2020 IEEE

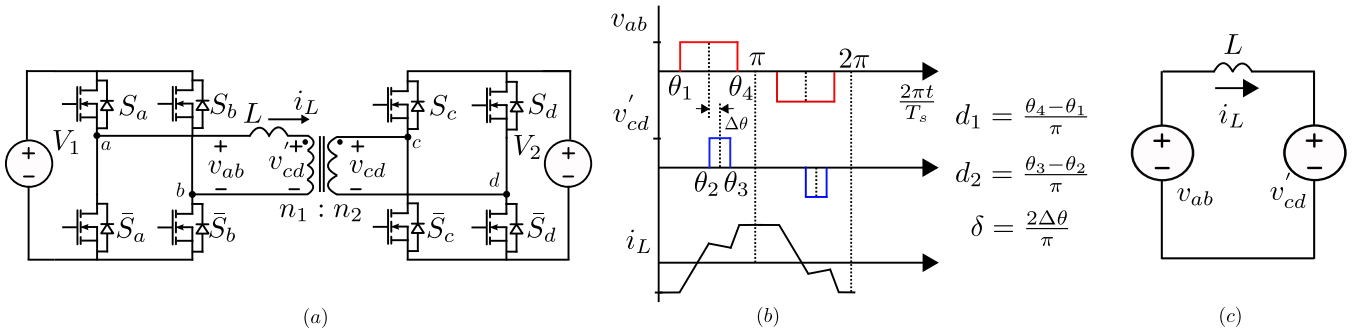

Fig. 1. (a) A DAB converter (b) Typical waveform with 3-DOF control (c) Equivalent circuit representation

as shown in Fig.1a. The H-bridge converters produce duty modulated square waveforms which are applied to the transformer with a given turns ratio $n_1 : n_2$ connected in series with an inductor L. Power transfer between the DC ports is carried out by introducing a phase shift, δ between v_{ab} and v_{cd}. Considering duty modulation of both primary and secondary voltage waveforms and the phase shift between them, there are three degrees of freedom in modulation viz. d_1, d_2 and δ as seen in Fig.1b. The magnetizing inductance is neglected and all the switches are considered ideal for the simplicity of analysis. The converter can thus be equivalently replaced by two voltage sources and an inductor L as shown in Fig.1c. The inductor current dynamics can be described by the following equation

$$L\frac{di_L}{dt} = v_{ab} - v_{cd}^{'} \tag{1}$$

To make the analysis independent of converter specifications, a per unit system is defined with voltage base as V_1 and current base as $\frac{V_1}{2\pi f_s L}$. The voltage conversion ratio m is defined as follows.

$$m = \frac{n_1 V_2}{n_2 V_1} \tag{2}$$

With the chosen current base, the per-unit inductor current i and hence the per-unit rms current i_{rms} will become a function of only m, d_1, d_2 and δ. Similarly, the per-unit average transferred power p is a function of only m, d_1, d_2 and δ. It is desired to operate the converter to minimise the losses. Accordingly, the inductor rms current should be minimised for a given per-unit power transfer $p_o = P \times \frac{2\pi f_s L}{V_1^2}$ while ensuring all the switching transitions are soft (ZVS) [5]. The problem can be mathematically formulated as in (3).

$$\min_{\substack{m>0,\ p=p_o \\ 0\le d_1,d_2,\delta\le 1,\ \text{ZVS}}} \quad i_{rms} \tag{3}$$

The ZVS conditions provide a set of inequality constraints based on the current polarities at the switching instants. For minimising the current stress through the devices, the peak or maximum magnitude of the instantaneous inductor current ($max(|i|)$) should be minimised for a given per-unit power transfer p_o, (4). Soft-switching should be ensured to minimise losses.

$$\min_{\substack{m>0,\ p=p_o \\ 0\le d_1,d_2,\delta\le 1,\ \text{ZVS}}} \quad max(|i|) \tag{4}$$

In this paper, solution of the rms and peak current optimisation problem is discussed for forward power transfer ($\delta > 0$). The reverse power transfer leads to identical solutions if the role of ports 1 and 2 are exchanged. For the various $[d_1, d_2, \delta] \in (0, 1)$, the converter can operate in five different zones where expressions of power, rms current and peak current are different. The expressions for power, rms currents and peak currents can be found in [4], [6].

A. Optimisation problem solution

The rms and peak current optimisation problem with the equality and inequality constraints described above can be solved through Karush-Kuhn-Tucker (KKT) conditions. For any given m, p_o should lie between 0 and $m\pi/4$, where $m\pi/4$ is the maximum possible per-unit power that can be transferred. For $m \le 1$, solution of the peak current optimisation problem leads to two zones depending on the value of operating power p_o. For p_o between 0 and p_{c1} (given in Table I), the converter operates with the optimum parameters d_1, d_2 and δ as shown in Table II (first column) [6]. For $p_o \in [p_{c1}, m\pi/4]$, the converter operates with a different set of optimal parameters (second column). The solution for $m > 1$ can be obtained similarly and is mentioned in Table II [6].

Solution of the rms current minimisation problem leads to three operating zones [5]. For power levels upto p_{c1}, the converter operates with the optimum parameters which are same as the peak current minimisation problem solution provided that $d_1 = md_2$. For $p_o \in [p_{c1}, p_{c2}]$, $d_2 = 1$ if $m \le 1$ and $d_1 = 1$ if $m > 1$ which means one of the bridges operate with square wave modulation. The optimal modulation parameters can be obtained by solving implicit equations in d_1 and δ for $m \le 1$ and in d_2 and δ for $m > 1$ (Table II, third column). For $p_o \in [p_{c2}, m\pi/4]$, the converter operates with single phase shift (SPS) strategy ($d_1 = d_2 = 1$) (Table II, fourth column). The rms and peak current expressions for the optimal strategy are given in Table III.

TABLE I
BOUNDARY POWER LEVELS [5], [6]

	p_{c1}	p_{c2}
$m \le 1$	$\frac{\pi m^2(1-m)}{2}$	$\frac{(1-m^2)\pi}{2m}\left(-1+\frac{1}{\sqrt{(1-m^2)}}\right)$
$m > 1$	$\frac{\pi(m-1)}{2m}$	$\frac{m\pi}{2}\left(1-m^2+m\sqrt{m^2-1}\right)$

TABLE II
OPTIMUM MODULATION PARAMETERS FOR RMS AND PEAK CURRENT MINIMIZATION [5], [6]

	Peak current optimisation solution (A)		**RMS current optimisation solution (B)**	
	$p_o \in [0, p_{c1})$	$p_o \in \left[p_{c1}, \frac{m\pi}{4}\right]$	$p_o \in [p_{c1}, p_{c2})$	$p_o \in \left[p_{c2}, \frac{m\pi}{4}\right]$
$m \leq 1$	$d_1 = \sqrt{\frac{2p_o}{(1-m)\pi}}$ $d_1 \leq m d_2$ $\delta = \frac{(1-m)d_1}{m}$	$d_1 = 1 - \sqrt{\left(1 - \frac{4p_o}{m\pi}\right)\frac{(1-m)^2}{(1-m)^2+m^2}}$ $d_2 = 1$ $\delta = 1 - \sqrt{2d_1 - d_1^2 - \frac{4p_o}{m\pi}}$	$\pi d_1(1-\delta) = \pi m\left(2d_1 - d_1^2\right) - 2p_o$ $d_2 = 1$ $\delta = 1 - \sqrt{2d_1 - d_1^2 - \frac{4p_o}{m\pi}}$	$d_1 = 1$ $d_2 = 1$ $\delta = 1 - \sqrt{1 - \frac{4p_o}{m\pi}}$
$m > 1$	$m d_2 \leq d_1$ $d_2 = \sqrt{\frac{2p_o}{\pi m(m-1)}}$ $\delta = (m-1)d_2$	$d_1 = 1$ $d_2 = 1 - \sqrt{\left(1 - \frac{4p_o}{m\pi}\right)\frac{(m-1)^2}{(m-1)^2+1}}$ $\delta = 1 - \sqrt{2d_2 - d_2^2 - \frac{4p_o}{m\pi}}$	$d_1 = 1$ $\pi d_2(1-\delta) = \frac{\pi}{m}\left(2d_2 - d_2^2\right) - \frac{2p_o}{m^2}$ $\delta = 1 - \sqrt{2d_2 - d_2^2 - \frac{4p_o}{m\pi}}$	$d_1 = 1$ $d_2 = 1$ $\delta = 1 - \sqrt{1 - \frac{4p_o}{m\pi}}$

TABLE III
RMS AND PEAK CURRENT EXPRESSIONS WITH OPTIMAL MODULATION STRATEGY

	Peak current	**RMS current for $p_o \leq p_{c1}$**	**RMS current for $p_o \geq p_{c1}$**
$m < 1$	$\frac{\pi}{2}\left(d_1 - m d_1 + m\delta\right)$	$\frac{\pi^2}{12}\left({d_1}^3 m - 2{d_1}^3 + 3{d_1}^2 d_2 m - 6 d_1 d_2 m + 3 d_1 \delta^2 m - 2{d_2}^3 m^2 + 3{d_2}^2 m^2\right)$	$\frac{\pi^2}{12}\left(-2{d_1}^3 - 3{d_1}^2\delta m + 3{d_1}^2 m + 3{d_1}^2 + 6 d_1\delta m - 6 d_1 m - 2{d_2}^3 m^2 - 3{d_2}^2\delta m + 3{d_2}^2 m^2 + 3{d_2}^2 m + 6 d_2\delta m - 6 d_2 m - \delta^3 m + 3\delta^2 m - 6\delta m + 4m\right)$
$m \geq 1$	$\frac{\pi}{2}\left(\delta - d_2 + m d_2\right)$	$\frac{\pi^2}{12}\left(-2{d_1}^3 + 3{d_1}^2 d_2 m + 3{d_1}^2 - 6 d_1 d_2 m - 2{d_2}^3 m^2 + {d_2}^3 m + 3{d_2}^2 m^2 + 3 d_2 \delta^2 m\right)$	

B. Closed form solution for medium power

The optimal modulation variables have an explicit formula for computation in all regions except for medium power operation ($p \in [p_{c1}, p_{c2}]$). For $m > 1$, the following equation needs to be solved to determine d_2.

$$2p_o + \pi m\left(d_2^2 - 2d_2\right) + m^2\pi d_2\sqrt{2d_2 - d_2^2 - \frac{4p_o}{m\pi}} = 0 \quad (5)$$

An explicit formula for evaluating d_2 is not available in literature. Existing techniques rely on software tools and curve fit techniques which makes the implementation complex and time consuming [4]. A technique to obtain closed form analytical expression for d_2 is proposed here. Rearranging the terms in (5) and squaring both sides, we obtain a *quartic equation* in d_2 (6) where the coefficients a, b, c and d are functions of m and p_o. Following a similar process for $m \leq 1$, a similar quartic equation in d_1 is obtained (7).

The closed form solution for d_2 (or d_1) can be obtained by solving the fourth order equation (6) (or (7)). Ferrari method is used for solution of (6) and (7). Evaluating the discriminant of the quartic equation reveals that it has two complex conjugate roots which are invalid solutions [12]. Only one of the roots lie in the range $[0, 1]$ which is the final solution of the equation. This root x can be either d_1 or d_2 and is given by [13],

$$x = \frac{-b}{4a} + S - \frac{1}{2}\sqrt{-4S^2 - 2t - \frac{q}{S}} \quad (8)$$

Calculation of the intermediate variable S, t and q in (8) is provided in (9), (10) and (11). The detailed technique can be found in [13].

$$t = \frac{8ac - 3b^2}{8a^2}, \qquad q = \frac{b^3 - 4abc - 8a^2 d}{8a^3} \quad (9)$$

$$\Delta_1 = 2c^3 - 9bcd + 27b^2 e + 27ad^2 - 72ace, \qquad \Delta_0 = c^3 - 3bd + 12ae \quad (10)$$

$$Q = \sqrt[3]{\frac{\Delta_1 + \sqrt{\Delta_1^2 - 4\Delta_0^3}}{2}}, \qquad S = \frac{1}{2}\sqrt{-\frac{2}{3}t + \frac{1}{3a}\left(Q + \frac{\Delta_0}{Q}\right)} \quad (11)$$

It can be observed that (8) requires time consuming math operations which may be challenging for real-time implementation. A modulation strategy is proposed to avert this problem and achieve other advantages.

C. Proposed optimal modulation strategy

1) Modulation strategy for $m = 1$: From Table I & II, it is possible to observe that for $m = 1$, $p_{c1} = p_{c2} = 0$. This means, the converter always operates with simple phase shift (SPS) modulation strategy. Thus, the optimal rms and peak are identical to that obtained for the SPS strategy.

$$\underbrace{\pi^2(1+m^2)}_{a}\boldsymbol{d_2^4} + \underbrace{2\pi^2(-2-m^2)}_{b}\boldsymbol{d_2^3} + \underbrace{\left(4\pi^2 + 4\pi m p_o + \frac{4\pi p_o}{m}\right)}_{c}\boldsymbol{d_2^2} \underbrace{-\frac{8\pi}{m}}_{d}\boldsymbol{d_2} + \underbrace{\frac{4p_o^2}{m^2}}_{e} = 0 \quad (6)$$

$$\underbrace{\pi^2(1+m^2)}_{a}\boldsymbol{d_1^4} + \underbrace{2\pi^2(-1-2m^2)}_{b}\boldsymbol{d_1^3} + \underbrace{\left(4\pi^2 m^2 + 4\pi m p_o + \frac{4\pi p_o}{m}\right)}_{c}\boldsymbol{d_1^2} \underbrace{-8\pi m p_o}_{d}\boldsymbol{d_1} + \underbrace{4p_o^2}_{e} = 0 \quad (7)$$

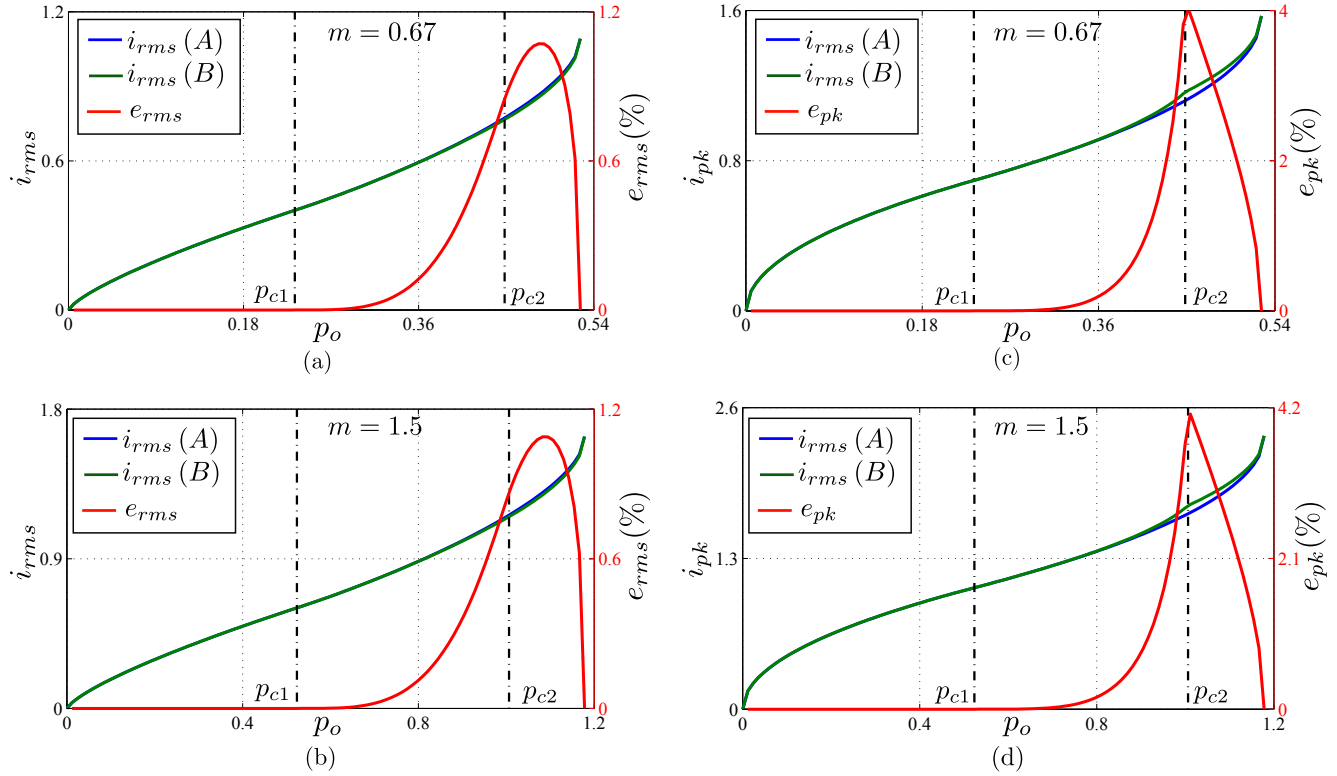

Fig. 2. Comparison of rms currents for solutions (A),(B) (a) $m = 0.67$, (b) $m = 1.5$, peak current comparison for solutions (A),(B) at (c) $m = 0.67$, (d) $m = 1.5$

2) Modulation strategy for $m \neq 1$: **(A)** denotes optimal solution for peak current minimisation for a given m and p_o. **(B)** similarly denotes the optimal solution for rms current minimisation.

Strategy for low power: For $p \in [0, p_{c1}]$, the peak and rms current optimisation problem lead to identical solutions which when used lead to both optimal rms and peak operation. So for this power range, use the solutions in the first column of Table I.

Strategy for medium power: For $p_{c1} \leq p_o < p_{c2}$, the rms obtained by using peak current optimal solution **(A)** is very close to the optimum rms currents obtained using **(B)** for $m < 1$ (Fig.2a) and $m > 1$ (Fig.2b). Since the peak current optimised solution is much simpler to implement, using the solution in this region leads to minimum peak current and near optimal rms currents. Defining the relative difference between the two rms currents as e_{rms}.

$$e_{rms} = \frac{i_{rms}(A) - i_{rms}(B)}{i_{rms}(B)} \times 100 \tag{12}$$

This factor is seen to be less than 1.2% for $m = 0.67$ and $m = 1.5$ (Fig.2a-b, red trace).

(c) Strategy for high power: For $p \geq p_{c2}$, rms current solution gives SPS modulation strategy which is simple to implement and leads to near optimal peak currents which can be observed in Fig.2c-d. Defining the relative difference between the two peak currents as e_{pk}.

$$e_{pk} = \frac{i_{pk}(B) - i_{pk}(A)}{i_{pk}(A)} \times 100 \tag{13}$$

This factor is less than 4% for $m = 0.67$ and less than 4.2% for $m = 1.5$ (Fig.2c-d, red trace). The rms currents are same as the global optimum rms currents in this region.

Fig.3 show the variation of the maximum values of factors e_{rms} and e_{pk} with m. It can be seen that at $m = 1$, the optimal rms and peak optimisation problems lead to identical (SPS) strategy. Thus, the values of e_{pk} and e_{rms} are zero. As the value of m deviates from unity, the relative difference in peak current e_{pk} increases. Thus, the hybrid modulation strategy with SPS in high power region gives sub-optimal peak current values for m far from unity. The maximum value of e_{rms} however stays within 2% for $m \in [0.5, 2]$. Thus, the proposed modulation strategy using both optimum rms and

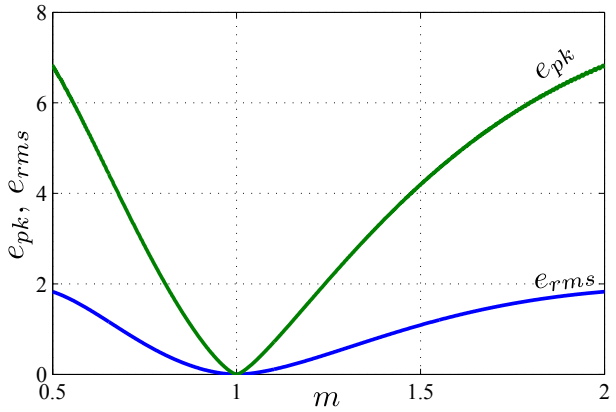

Fig. 3. Variation of e_{pk} and e_{rms} with m

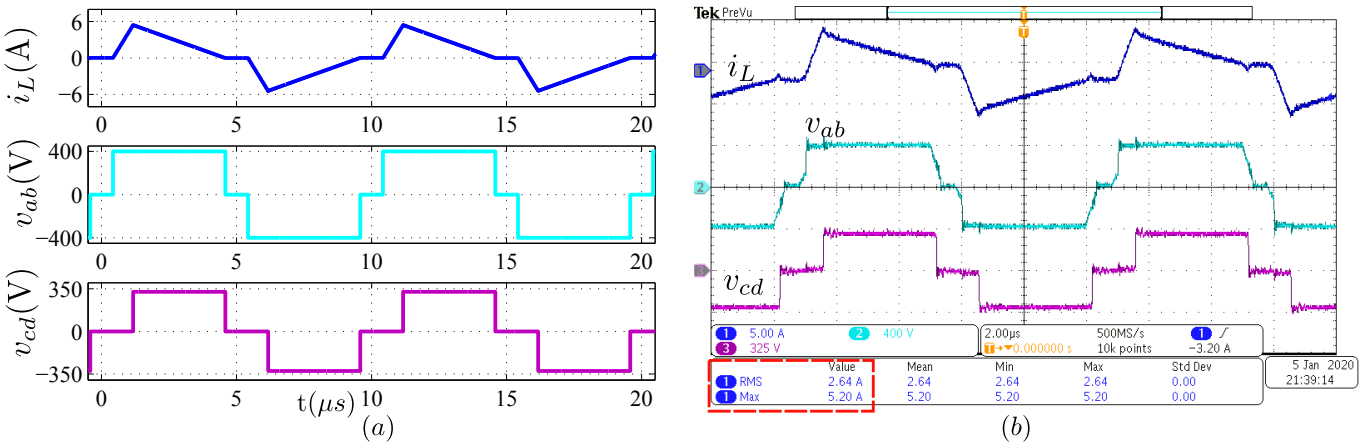

Fig. 4. Simulation and experimental results at low power (0.9 kW)

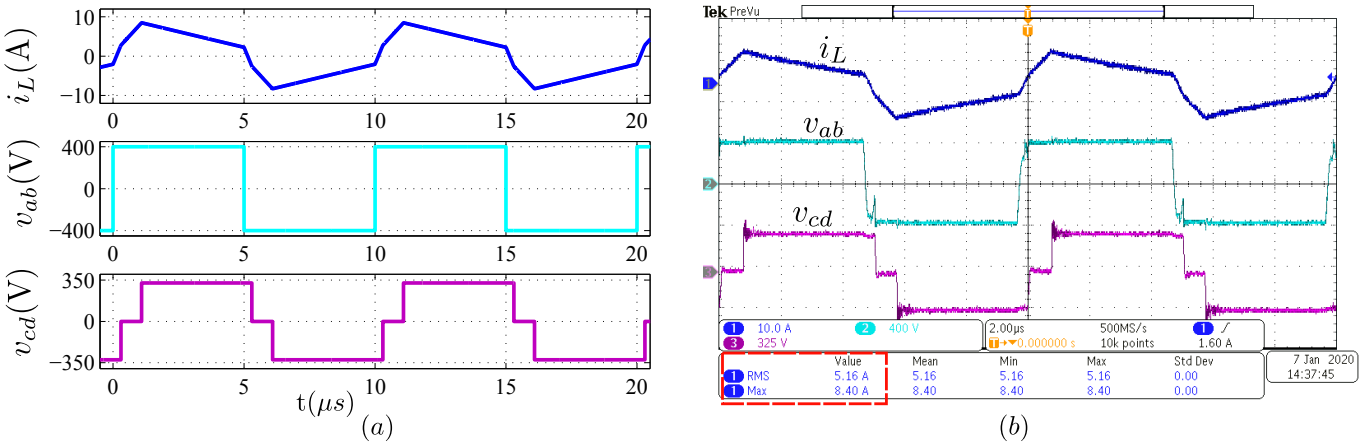

Fig. 5. Simulation and experimental results at medium power (2.0 kW)

peak current solution leads to simplicity of implementation and optimal operation of the converter.

III. Simulation and Experimental Results

The validity of the proposed modulation technique is verified on an experimental prototype with the ratings given in Table IV. The experimental set-up is shown in Fig.6. $V_1 = 400$V, $V_2 = 325$V, $P = 4$kW, $f_s = 100$kHz, $L = 55.2\mu H$ and $n = 1.5$. This results in $m = 1.22$ and the power boundaries $P_{c1} = 1.3$kW and $P_{c2} = 3.2$kW. The component specifications used in the hardware set-up are provided in Table VI. The converter operation is simulated in MATLAB/Simulink and is experimentally validated at low (0.9kW), medium (2kW) and high (3.3kW) operating powers. Simulation and experimental results for low, medium and high power operation are shown in Fig. 4, 5 and 7 respectively.

TABLE IV
Hardware Specifications

V_1	V_2	P	L	n	f_s
400 V	325 V	4 kW	55.2μH	1.5	100 kHz

A comparison of the theoretical simulation and experimental results is provided in Table V.

The simulation and experimental results (with rms and peak currents) for low power operation are shown in Fig.4. For low power operation, $d_1 = 0.83$, $d_2 = 0.68$, $\delta = 0.15$ is obtained from Table II. The rms and peak current can be calculated to be 2.85A and 5.41A respectively. For medium power operation (Fig.5), the peak current optimal solution is

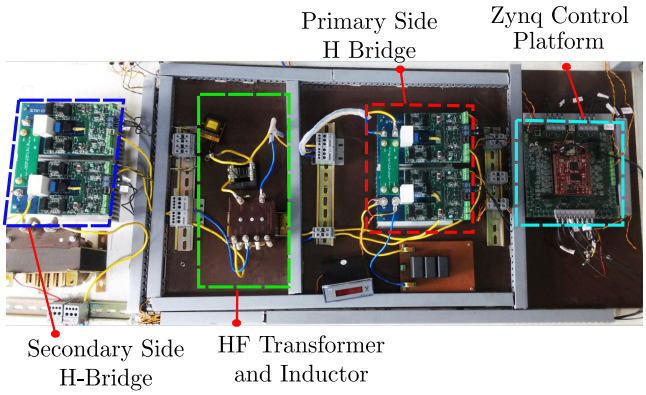

Fig. 6. Experimental Set-up

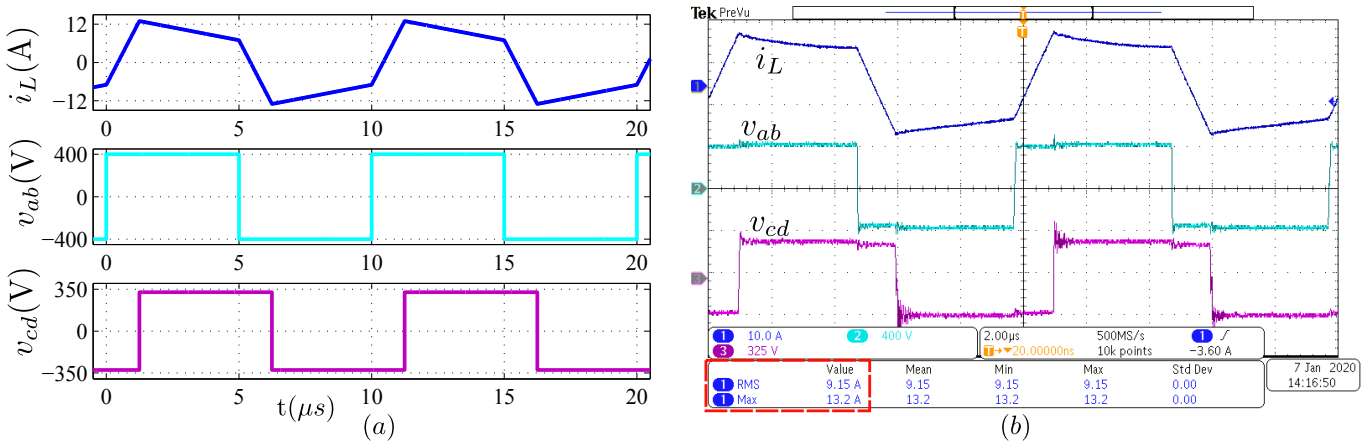

Fig. 7. Simulation and experimental results at high power (3.3 kW)

TABLE V
COMPARISON AT FOUR OPERATING POINTS OF CONVERTER

	P (kW)	(d_1, d_2, δ)	I_{rms} (th.)	I_{pk} (th.)	I_{rms} (sim.)	I_{pk} (sim.)	I_{rms} (exp.)	I_{rms} (exp.)
Low	0.9	(0.83, 0.68, 0.15)	2.85	5.41	2.84	5.41	2.64	5.20
Med	2.0	(1, 0.84, 0.28)	5.43	8.36	5.44	8.40	5.16	8.40
High	3.3	(1, 1, 0.49)	9.37	12.97	9.38	13.00	9.15	13.20

TABLE VI
COMPONENT LIST

Part	**Part Number**	**Rating**
Switches	SCH2080KE	1200V 28A
Gate Driver	ADuM4135	Iso. driver
Capacitor $C_1 - C_2$	C4ASPBW4250A3MJ	2.5μF × 2

used ($d_1 = 1$, $d_2 = 0.84$, $\delta = 0.28$), with $i_{rms} = 5.43$A and $i_{pk} = 8.36$A. For high power operation, the rms current optimal solution is used (Fig.7) ($d_1 = d_2 = 1$ and $\delta = 0.49$) with $i_{rms} = 9.37$A and $i_{pk} = 12.97$A. A close agreement between the theoretical, simulation and experimental values (shown in Table V) is obtained for all the operating powers.

IV. CONCLUSION

This paper presented a comparative study between the optimal modulation strategies for achieving minimum inductor rms and peak currents. A closed-form solution technique is also proposed for determining the optimal modulation variables for medium power operation which leads to minimum rms currents. A modulation strategy is proposed which leads to overall minimisation of both rms and peak currents. For medium power operation, the peak current solution is used which gives minimum peak current and near optimal rms currents. This solution is much simpler when compared to rms current optimal solution. For high power operation, a simple strategy is used which gives optimal rms current but near optimal peak currents.

REFERENCES

[1] R. De Doncker, D. Divan, and M. Kheraluwala, "A three-phase soft-switched high-power-density dc/dc converter for high-power applications," *IEEE Trans. on Ind. Electron.*, vol. 27, no. 1, pp. 63–73, 1991.

[2] M. Kheraluwala, R. Gascoigne, D. Divan, and E. Baumann, "Performance characterization of a high-power dual active bridge dc-to-dc converter," *IEEE Trans. on Ind. Electron.*, vol. 28, no. 6, pp. 1294–1301, 1992.

[3] A. K. Jain and R. Ayyanar, "PWM control of dual active bridge: Comprehensive analysis and experimental verification," *IEEE Trans. on Power Electron.*, vol. PP, no. 99, p. 1, 2010.

[4] F. Krismer and J. Kolar, "Closed form solution for minimum conduction loss modulation of DAB converters," *IEEE Trans. on Power Electron.*, vol. 27, no. 1, pp. 174–188, 2012.

[5] A. Tong, L. Hang, G. li, X. jiang, and S. Gao, "Modeling and analysis of dual-active-bridge isolated bidirectional dc/dc converter to minimize rms current with whole operating range," *IEEE Trans. Power Electron.*, vol. PP, no. 99, pp. 1–1, 2017.

[6] S. Shao, M. Jiang, W. Ye, Y. Li, J. Zhang, and K. Sheng, "Optimal phase-shift control to minimize reactive power for a dual active bridge dc–dc converter," *IEEE Trans. on Power Electron.*, vol. 34, no. 10, pp. 10 193–10 205, Oct 2019.

[7] N. Hou, W. Song, and M. Wu, "Minimum-current-stress scheme of dual active bridge dc–dc converter with unified phase-shift control," *IEEE Trans. on Power Electron.*, vol. 31, no. 12, pp. 8552–8561, Dec 2016.

[8] Q. Gu, L. Yuan, J. Nie, J. Sun, and Z. Zhao, "Current stress minimization of dual-active-bridge dc–dc converter within the whole operating range," *IEEE Journal of Emerging and Selected Topics in Power Electronics*, vol. 7, no. 1, pp. 129–142, March 2019.

[9] J. Huang, Y. Wang, Z. Li, and W. Lei, "Unified triple-phase-shift control to minimize current stress and achieve full soft-switching of isolated bidirectional dc–dc converter," *IEEE Trans. on Ind. Electron.*, vol. 63, no. 7, pp. 4169–4179, July 2016.

[10] B. Zhao, Q. Song, W. Liu, and W. Sun, "Current-stress-optimized switching strategy of isolated bidirectional dc–dc converter with dual-phase-shift control," *IEEE Trans. on Ind. Electron.*, vol. 60, no. 10, pp. 4458–4467, Oct 2013.

[11] C. Song, A. Chen, J. Chen, C. Du, and C. Zhang, "Optimized modulation scheme for dual active bridge dc-dc converter," in *2018 IEEE Applied Power Electronics Conference and Exposition (APEC)*, March 2018, pp. 3569–3574.

[12] L. Euler, "Of a new method of resolving equations of the fourth degree," in *Elements of Algebra*. Springer, 1972, pp. 282–288.

[13] A. G. Kurosh, *A course in higher algebra*, 1975.